The Journal of Physiology

# Systemic histone deacetylase inhibition ameliorates the aberrant responses to acute stress in socially isolated male mice

Luis Gustavo Hernandez Carballo, Pei Li, Rachel Senek and Zhen Yan

*Department of Physiology and Biophysics, Jacobs School of Medicine and Biomedical Sciences, State University of New York at Buffalo, Buffalo, NY, USA*

Handling Editors: David Wyllie & Conny Kopp-Scheinpflug

The peer review history is available in the Supporting Information section of this article (https://doi.org/10.1113/JP285875#support-information-section).

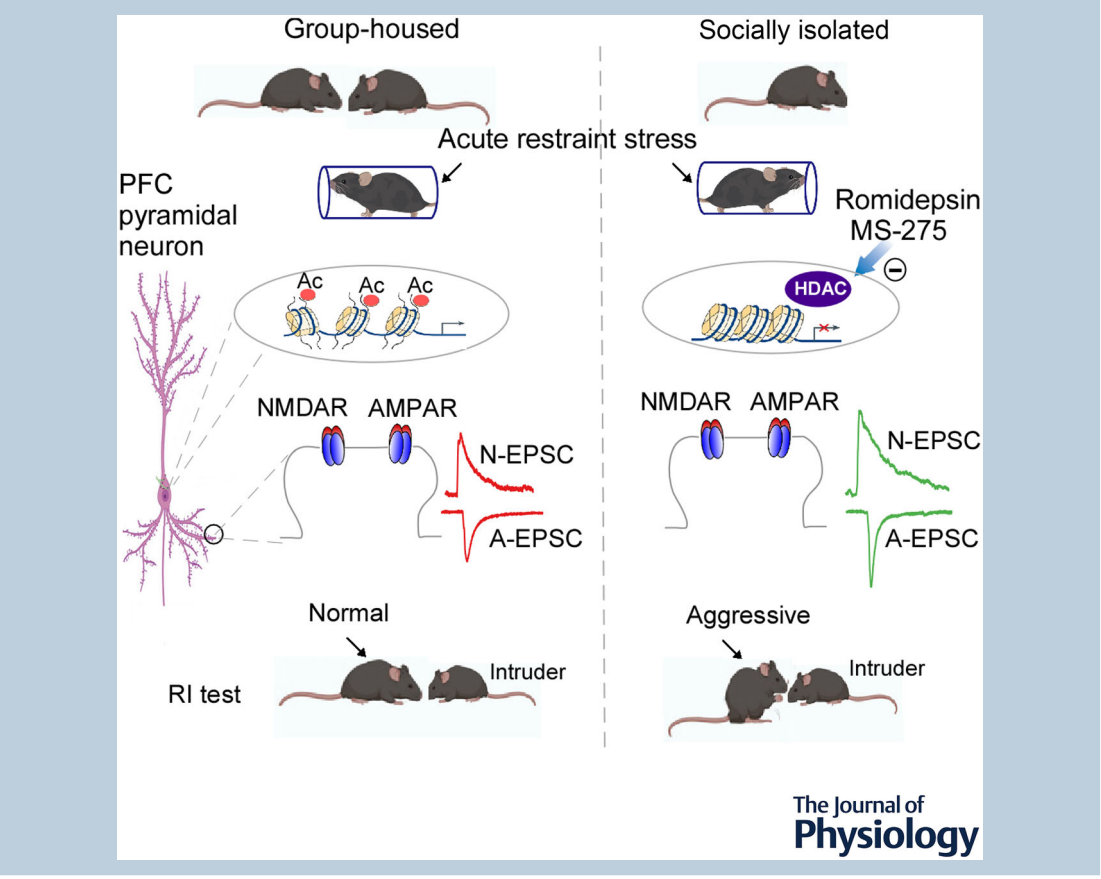


**Luis Gustavo Hernandez Carballo** is currently a Postdoctoral Fellow in State University of New York at Buffalo, School of Medicine and Biomedical Sciences. He earned Master's and PhD degrees in Physiological Sciences from Benemérita Universidad Autónoma De Puebla in Mexico. His research centred primarily around the synaptic action of neuromodulators associated with mental health and illnesses. He has over 10 years of experience in electrophysiological techniques and data analysis tool development. Recently, he has been investigating epigenetic abnormalities caused by genetic and environmental factors, contributing to synaptic dysfunction and behavioural deficits.



DOI: 10.1113/JP285875

**Abstract** Adverse experiences in early life can induce maladaptive responses to acute stress in later life. Chronic social isolation during adolescence is an early life adversity that can precipitate stress-related psychiatric disorders. We found that male mice after 8 weeks of adolescent social isolation (SI) have markedly increased aggression after being exposed to 2 h of restraint stress (RS), which was accompanied by a significant increase of AMPA receptor- and NMDA receptor-mediated synaptic transmission in prefrontal cortex (PFC) pyramidal neurons of $SI^{RS}$ males. Compared to group-housed counterparts, $SI^{RS}$ males exhibited a significantly decreased level of histone H3 acetylation in PFC. Systemic administration of class I histone deacetylase inhibitors, romidepsin or MS-275, ameliorated the aggressive behaviour, as well as general social interaction deficits, of $SI^{RS}$ males. Electrophysiological recordings also found normalization of PFC glutamatergic currents by romidepsin treatment of $SI^{RS}$ male mice. These results revealed an epigenetic mechanism and intervention avenue for aggression induced by chronic social isolation.

(Received 29 October 2023; accepted after revision 1 March 2024; first published online 18 March 2024)
**Corresponding author** Z. Yan: Department of Physiology and Biophysics, Jacobs School of Medicine and Biomedical Sciences, State University of New York at Buffalo, Buffalo, NY 14203, USA. Email: zhenyan@buffalo.edu

**Abstract figure legend** Schematic diagram showing a potential mechanism underlying the aberrant response to acute stress in socially isolated male mice. Group-housed or single-housed (8 weeks, starting at 3 weeks old) mice were exposed to an acute (2 h) restraint stress, followed by behavioural assays. Chronically isolated mice exhibited dramatically heightened aggression in the resident–intruder (RI) test, which was accompanied by the decreased histone acetylation and increased synaptic currents mediated by NMDA and AMPA receptors in pyramidal neurons of the prefrontal cortex (PFC). Treatment with class I histone deacetylase (HDAC) inhibitors, romidepsin or MS-275, normalized PFC glutamatergic currents, and ameliorated the aggressive behaviour of isolation-reared male mice.

**Key points**

- Adolescent chronic social isolation can precipitate stress-related psychiatric disorders.
- A significant increase of glutamatergic transmission is found in the prefrontal cortex (PFC) of socially isolated male mice exposed to an acute stress ($SI^{RS}$).
- Treatment with class I histone deacetylase (HDAC) inhibitors ameliorates the aggressive behaviour and social interaction deficits of $SI^{RS}$ males, and normalizes glutamatergic currents in PFC neurons.
- It provides an epigenetic mechanism and intervention avenue for aberrant stress responses induced by chronic social isolation.

## Introduction

Social interactions play a causal role in determining health and survival in humans and other animals because of their direct impact on physiology, disease risk and lifespan (Kendler et al., 1999; Snyder-Mackler et al., 2020). Chronic social isolation during adolescence is recognized as an early life adversity that can precipitate stress-related psychiatric disorders (Almeida et al., 2021; Hawkley & Cacioppo, 2010). Emotional abnormalities resulting from early social neglect include anxiety, depression and excessive aggression (Haller et al., 2014; Tan et al., 2021; Wang et al., 2022; Zelikowsky et al., 2018). Adverse experiences in early life can also induce maladaptive responses to acute stress in later life (Holz et al., 2023; Nemeroff, 2016).

The complex interplay between genetic and environmental factors plays a crucial role in stress-induced mental disturbances (Barnett Burns et al., 2018; Rahman & McGowan, 2022; Waltes et al., 2016). One mechanism that has come into focus for mediating this interplay is epigenetics, which refers to a collection of gene regulatory processes through histone modification or DNA methylation to dynamically regulate chromatin structure and transcriptional accessibility (Strahl & Allis, 2000; Wu & Zhang, 2014). Epigenetic modifications induced by early life stress (ELS) can shape the molecular response of a cell to its environment as a function of genetic predisposition (Klengel & Binder, 2015). A persistent histone acetylation increase has been revealed in the nucleus accumbens of mice exposed to chronic social defeat stress (Covington et al., 2009). In two

genetically distinct mouse strains, the susceptibility or adaptation to chronic stress is determined by differential epigenetic changes in the *Gdnf* promoter to either repress or activate *Gdnf* transcription (Uchida et al., 2011). Adult male mice exposed to social isolation stress exhibit increased global DNA methylation and enhanced activity of DNA methyltransferase in the midbrain, as well as activation of histone acetyltransferases and histone deacetylases (Hdac1 and Hdac3) and alteration of histone H3 lysine 9 acetylation (Siuda et al., 2014). These stress-induced epigenetic changes may mediate neuronal positive adaptation or negative maladaptation.

In this study, we sought to elucidate the altered behavioural response to acute stress in adult male mice after adolescent social isolation, as well as the underlying physiological alteration in key brain regions controlling emotional processes, such as the prefrontal cortex (PFC) (Yan & Rein, 2022). Moreover, we examined the therapeutic potential of targeting epigenetic enzymes for behavioural and physiological aberrations induced by adolescent social isolation.

## Materials and methods

### Animal and regents

All experiments were performed with the approval of the Institutional Animal Care and Use Committee (IACUC) of the State University of New York at Buffalo (PROTO202000049). C57BL/6J mice were bred and maintained in our institutional animal facility under controlled environmental conditions (22°C, 12 h light/dark cycle) with free access to food and water. Romidepsin (Selleck Chemicals, Houston, TX, USA), UNC0642 (Tocris, Ellisville, MO, USA) and MS-275 (Selleck Chemicals) were dissolved in DMSO and then diluted with 0.9% saline before use. DMSO concentration of the working solution was <0.5%. Mice were treated systemically (I.P.) with romidepsin (1 mg/kg), MS-275 (5 mg/kg), UNC0642 (1 mg/kg) or vehicle (saline containing 0.5% DMSO) once daily for three consecutive days.

### Social isolation and acute stress protocol

Similar to what was previously described (Chang et al., 2015; Tan et al., 2021; Wang et al., 2022), post-weaning social isolation (SI) was carried out from postnatal day 21 (P21) to P77 (8 weeks). The mice were randomly separated into group housing (GH, three or four mice per cage) or individual housing (one mouse per cage). Enrichment was removed for SI (Lukkes et al., 2009), and other husbandry conditions were the same as GH. All animals were housed with *ad libitum* food accessibility in the 12 h light–dark cycle (light: 06.00–18.00 h; dark: 18.00–06.00 h). For restraint stress, each mouse (P78–81) was placed in a plastic cylinder and restrained for 2 h. The acute stress was given 24 h before behavioural or electrophysiological measurements.

### Behavioural test

Animals (P79–82) were transferred to behavioural testing room (dim light) 1−2 h before testing. All behavioural experiments were carried out during the day (10.00–15.00 h). Animals were used to handling before testing.

**Elevated plus-maze (EPM) test.** Mice were placed in the centre of a plus maze that was elevated 50 cm above the floor with two opposite open arms and two opposite closed arms (each arm was 88 cm long, 28 cm high walls only on closed arms) arranged at right angles. The number of entries and time spent in the closed and open arms were monitored for 5 min.

**Resident–intruder (RI) test.** A modified protocol (Chang et al., 2015) was used. Briefly, the group-housed mice were individually housed for 1 day prior to the RI test, while the home cages of single-housed mice were not changed. In the RI test, the 'resident' mouse was exposed to an 'intruder', a slightly smaller (5–15% lighter) unfamiliar control mouse of the same sex, in the home cage for 10 min. The intruders were all socially experienced, but naive to the RI test. Each intruder was used only once and was not re-used for other aggressive encounters (to avoid winner or loser effects). Aggressive behaviour of the resident mouse against the intruder, including lateral threat, upright posture, clinch attack, keep down and chase (Lukkes et al., 2009; Miczek et al., 2001), were scored to measure the aggression level. The number and time of social interactions between the resident mouse and the intruder, as well as the locomotive activity of the resident mouse, were tracked using a custom software written on top of OpenCV in Python (Bradski, 2000). Non-aggressive interactions were calculated by subtracting aggressive events from total interactions.

### Immunocytochemical staining

Animals were anaesthetized with a mixture of ketamine/xylazine (100/10 mg/kg) before perfusion. After perfusion with 4% fresh prepared paraformaldehyde (PFA), brains were collected, post-fixed in 4% PFA overnight and dehydrated in 30% sucrose for 2 days. Brain slices (50 $\mu$m) containing mouse PFC, which consists of anterior cingulate cortex (ACC), prelimbic (PL), and infralimbic (IL), were cut coronally for staining. After

washing with PBS three times (10 min each), slices were blocked in PBS containing 5% bvine serum albumin (BSA (and 0.3% Triton for 2 h at room temperature. Then slices were incubated with primary antibody against H3K9Ac (1:1000, Cell Signaling Technology, Danvers, MA, USA; 9649) and NeuN (1:500, Millipore Sigma, Billerica, MA, USA; MAB 377) overnight at 4°C. After washing with PBS three times (15 min each), slices were incubated with secondary antibodies, Alexa Fluor 488-anti rabbit (1:1000, Invitrogen, Carlsbad, CA, USA; A-11008) and Alexa Fluor 568-anti mouse (1:1000, Invitrogen; A-11004), for 2 h at room temperature. DAPI (ThermoFisher, Waltham, MA, USA; D1306, 5 $\mu$g/ml) was used to stain nucleus for 30 min at room temperature. ProLong$^{TM}$ Diamond Antifade Mountant (Invitrogen; P36970) was used to prepare microscope slides. Images were acquired using a 63× objective on a Leica TCS SP8 confocal microscope. All specimens were imaged under identical conditions and analysed with identical parameters using ImageJ software (version 1.52p, NIH, Bethesda, MD, USA).

### Electrophysiological recording

Mice were decapitated under 1–3% isoflurane (Millipore Sigma, Burlington, MA, USA) anaesthesia and the brain was quickly removed and coronally cut into 300 $\mu$m slices with a vibratome (Leica VP1000S, Leica Microsystems Inc., Wetzlar, Germany) in an ice-cold sucrose solution. The slices were recovered and maintained at room temperature (22°C) in standard artificial cerebrospinal fluid (ACSF; in mM: 130 NaCl, 26 $NaHCO_3$, 3 KCl, 5 $MgCl_2$, 1.25 $NaH_2PO_4$, 1 $CaCl_2$, 10 glucose) for at least 1 h. The slice was transferred into a recording chamber on an upright microscope (Olympus) and perfused with oxygenated ACSF. Neurons were viewed under a water-immersion lens (40×) and a CCD camera. A Multiclamp 700 A amplifier with Clampex 8.2 software and Digidata 1322A (Molecular Devices, Sunnyvale, CA, USA) were used for recordings. A pipette puller (Model P-97, Sutter Instrument Co., Novato, CA, USA) was used to pull recording pipettes from glass capillaries (1.5 mm OD and 0.86 mm ID) with resistance at 3−4 MΩ.

Whole-cell voltage-clamp recording was used to measure synaptic currents in mouse PFC (ACC and PL) layer V pyramidal neurons (Tan et al., 2019; Wang et al., 2018). The pipette was filled with the intracellular solution (in mM: 130 caesium methanesulphonate, 10 CsCl, 4 NaCl, 1 $MgCl_2$, 10 HEPES, 5 EGTA, 2 QX-314, 12 phosphocreatine, 5 MgATP, 0.5 $Na_3GTP$, 0.1 leupeptin, pH 7.3, 270 mOsm). A stimulating electrode (FHC, Bowdoinham, ME, USA) was placed ∼100 $\mu$m away from the recorded neuron. EPSCs were elicited by a series of pulses from an S48 stimulator (Grass Technologies, West Warwick, RI, USA) with different intensities that delivered at 0.05 Hz. For input–output responses, EPSC was evoked by a series of pulses with different stimulation intensities (1−7 V) delivered at 0.05 Hz. For AMPA receptor (AMPAR)-EPSC, the membrane potential was maintained at −70 mV. For NMDA receptor (NMDAR)-EPSC, the cell (clamped at −70 mV) was depolarized to +40 mV for 3 s before stimulation to fully relieve voltage-dependent $Mg^{2+}$ block. The peak of NMDAR-EPSC was calculated at 40 ms after the onset of mixed EPSC when AMPAR was inactivated (Zhong et al., 2022). $GABA_A$ receptor ($GABA_A$R)-IPSC was recorded with a holding potential of 0 mV using the same internal solution. Spontaneous EPSCs (sEPSC) and IPSCs (sIPSCs) were recorded with the same external and internal solutions in neurons clamped at −70 and 0 mV, respectively.

### Statistics

A custom-made python script based on *Neo* (Garcia et al., 2014) was used for electrophysiological data analyses. Statistical analysis of the data was performed using the rstatix framework (Kassambara, 2022) for the R statistical software. All data were presented as means ± SEM. Experiments with two groups were analysed statistically using unpaired Student's *t* tests with Welch's correction, unless the data failed Shapiro–Wilk tests for normality, in which case the data were subjected to a Mann–Whitney *U* (M-W) test. Experiments with more than two groups were subjected to an ANOVA (one-way or repeated-measures two-way) or a Kruskal–Wallis test, followed by *post hoc* comparisons with Bonferroni corrections for multiple comparisons.

## Results

### Chronic social isolation leads to an aberrant behavioural response after acute stress

To determine the impact of chronic social isolation (SI) on the response to acute stress, we gave a 2 h restraint stressor (RS) to male mice either single housed for 8 weeks (starting at 3 weeks old) or group housed (GH) throughout rearing. First, we carried out an RI test, a paradigm with high face and construct validity for aggressive behaviours (Koolhaas et al., 2013). As shown in Fig. 1*A*, compared to $GH^{RS}$ control mice, $SI^{RS}$ mice exhibited a small but significant decrease in the number of total interactions, but a dramatic increase in the number and duration of aggressive interactions against intruders, suggesting a maladaptive response to acute stress, particularly the heightened aggression, consistent with previous findings (Chang et al., 2018; Nordman et al., 2020). Interestingly, the number of non-aggressive interactions was also significantly reduced in $SI^{RS}$ mice, suggesting the impairment of general social interaction. During RI tests, the locomotion

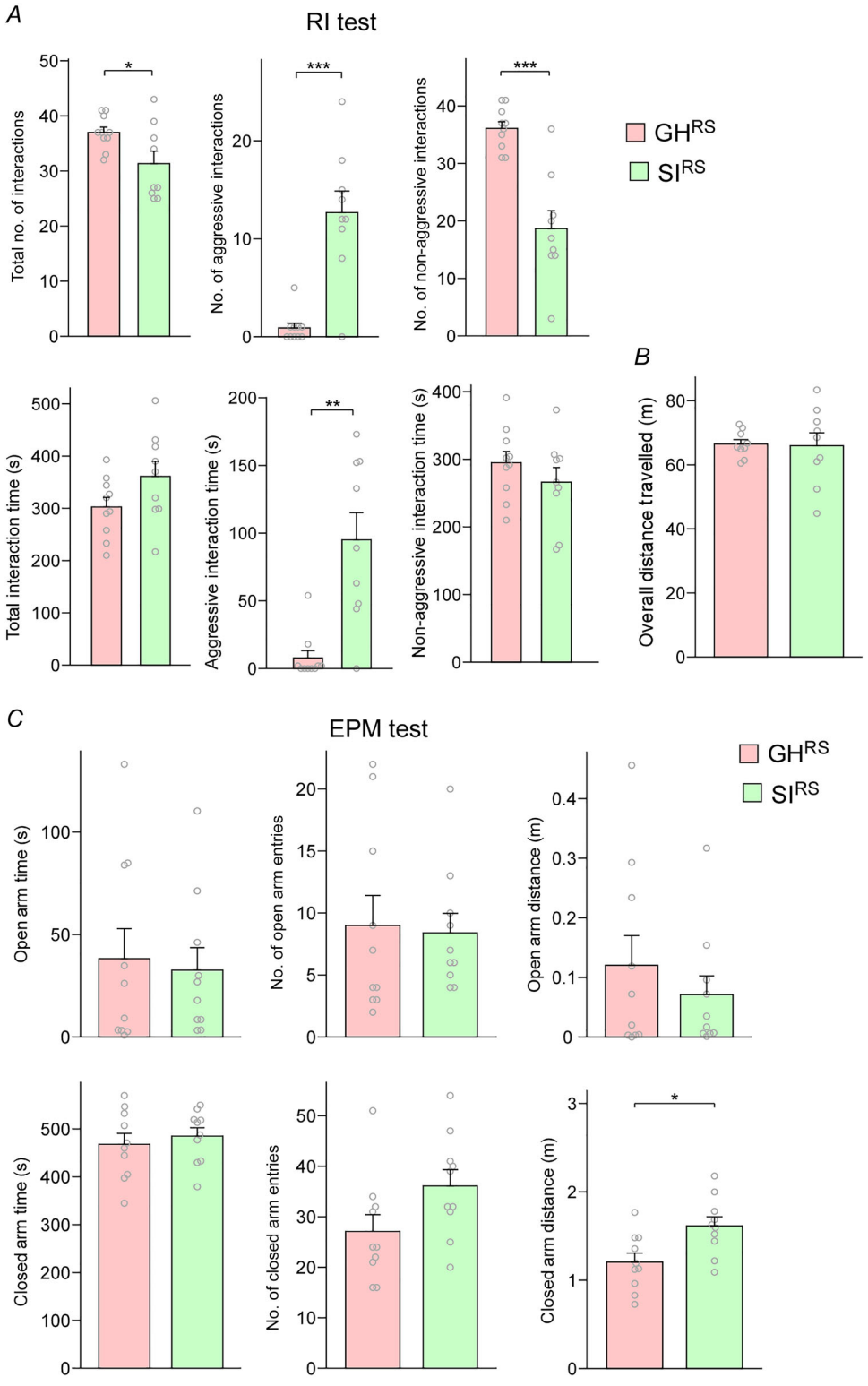


**Figure 1. Socially isolated male mice exposed to acute stress show escalated aggression**
*A*, bar graphs showing aggressive behaviour in the resident–intruder (RI) test of group-housed and single-housed socially isolated mice after an acute restraint stress ($GH^{RS}$ and $SI^{RS}$, $n$ = 9−10 mice per group; Total no. of interactions: $t_{11}$ = 2.3, $P$ = 0.04; No. of aggressive interactions: $t_9$ = 5.2, $P$ = 0.0006; No. of non-aggressive interactions: $t_{10}$ = 5.2, $P$ = 0.0004; Total interaction time: $t_{14}$ = 1.7, $P$ = 0.1; Aggressive interaction time: $t_9$ = 4.2, $P$ = 0.002; Non-aggressive interaction time: $t_{16}$ = 1.1, $P$ = 0.3, $t$ test). *B*, bar graphs of the overall distance travelled by each group while performing the RI test ($n$ = 9 mice per group; $t_{10}$ = 0.1; $P$ = 0.9, $t$ test). *C*, bar graphs of time, distance

travelled and number of entries to open arms (OA) and closed arms (CA) for both groups in the elevated plus maze (EPM) test ($n$ = 10 mice per group; OA time: $t_{17}$ = 0.3, $P$ = 0.8; CA time: $t_{17}$ = 0.6, $P$ = 0.6; OA distance: $t_{15}$ = 0.8, $P$ = 0.4; CA distance: $t_{18}$ = −2.8, $P$ = 0.01; OA entries: $t_{16}$ = 0.2, $P$ = 0.8; CA entries: $t_{18}$ = 2.0, $P$ = 0.07, $t$ test). In all figures, $^{*}P < 0.05$, $^{**}P < 0.01$, $^{***}P < 0.001$. All data are expressed as mean ± SEM.

of testing mice did not reveal significant differences between groups (Fig. 1*B*), suggesting that the aggressive behaviour of $SI^{RS}$ mice was not due to a locomotive abnormality.

Next, both groups were tested in the EPM, a widely used behavioural test to assess anxiety-related behaviours (Walf & Frye, 2007). As shown in Fig. 1*C*, $SI^{RS}$ and $GH^{RS}$ mice exhibited no significant differences on most parameters, including time in the open arm, open arm entry numbers and distance travelled on the open arm, suggesting that $SI^{RS}$ mice do not have apparent anxiety.

## Isolated mice exposed to acute stress have increased glutamatergic transmission in PFC pyramidal neurons

To determine what might be driving the aberrant response to acute stress in $SI^{RS}$ mice, we examined the synaptic activity in PFC, a brain region playing a key role in regulating stress-induced excessive aggressive behaviour (Nelson & Trainor, 2007; Zhang et al., 2022). Whole-cell patch-clamp recordings were performed to measure sEPSC and AMPAR- or NMDAR-mediated EPSC evoked by electrical stimulation, as well as spontaneous and evoked $GABA_A$R-mediated IPSCs in layer V PFC pyramidal neurons. Evoked synaptic currents reflect the integrated response from simultaneous activation of multiple synapses that have action potential-driven synchronous or asynchronous release of vesicles. Spontaneous synaptic currents reflect the response induced by randomly activated synapses that have action potential-independent release of single synaptic vesicles.

As shown in Fig. 2*A* and *B*, the amplitudes of NMDAR- and AMPAR-EPSC evoked by a series of stimulation intensities were significantly larger in $SI^{RS}$ mice compared to $GH^{RS}$ mice. The input/output curve of $GABA_A$R-IPSC was similar in $SI^{RS}$ *versus* $GH^{RS}$ mice (Fig. 2*C*). The amplitude or frequency of sEPSC or sIPSC was also not significantly different between the two groups (Fig. 2*D* and *E*). Taken together, these results indicate that the aberrant behavioural response to acute stress in $SI^{RS}$ mice is accompanied by an increase of AMPAR- and NMDAR-mediated synaptic transmission in PFC pyramidal neurons.

## HDAC inhibition rescues the aberrant behavioural response to acute stress in socially isolated male mice

Since the activity of class I histone deacetylases (HDACs) is upregulated after various forms of chronic stress (Covington et al., 2009; Siuda et al., 2014; Uchida et al., 2011), we also compared the level of histone acetylation in deep and intermediate layers of PFC subregions from group-housed *versus* socially isolated male mice after acute stress. As shown in Fig. 3*A* and *B*, the fluorescence signal of H3K9 acetylation (H3K9Ac) was significantly decreased in layer 5/6 ACC, layer 2/3 ACC and layer 2/3 PL neurons of $SI^{RS}$ mice, compared with $GH^{RS}$ mice. No significant changes of H3K9Ac were found in layer 5/6 IL and PL or layer 2/3 IL. When all the data were pooled, the fluorescence signals of H3K9Ac in layer 5/6 and layer 2/3 medial PFC neurons of $SI^{RS}$ mice were significantly lower than those from $GH^{RS}$ mice.

Next, we treated $SI^{RS}$ mice with a highly potent and brain-permeable class I HDAC inhibitor, romidepsin (0.25 mg/kg, I.P., 3×) (Qin et al., 2018; Zhang et al., 2021). Another structurally different class I HDAC inhibitor, MS-275 (5 mg/kg, I.P., 3×) (Ma et al., 2018), was also used to confirm the involvement of HDAC. Two hours after the 3 day treatment, animals were given an acute stressor, followed by behavioural testing the next day. As shown in Fig. 4*A*, compared to vehicle-treated controls ($SI^{RS}$+Veh), $SI^{RS}$ mice treated with romidepsin ($SI^{RS}$+Rom) exhibited a significant reduction in the number and time of aggressive interactions in the RI test, and $SI^{RS}$ mice treated with MS-275 ($SI^{RS}$+MS275) also had a significantly reduced aggressive interaction time. Interestingly, the reduced non-aggressive interactions in $SI^{RS}$ mice were improved by romidepsin or MS-275 treatment, suggesting their pro-social effects.

To determine the specificity of this therapeutic effect of HDAC inhibitors, we tested another epigenetic drug, UNC0642 (1 mg/kg, I.P., 3×) (Wang et al., 2021; Zheng et al., 2019), a highly selective and potent inhibitor of histone methyltransferase EHMT1/2. As shown in Fig. 4*A*, treatment with UNC0642 failed to reduce the numbers or time of aggressive interactions in $SI^{RS}$ mice, suggesting the lack of involvement of EHMT.

To ensure that the observed reduction of aggressive behaviour was not caused by drug-induced changes in locomotion, we tracked locomotor activity of mice during RI tests. No significant differences in locomotion were observed among $GH^{RS}$ or $SI^{RS}$ mice treated with vehicle, romidepsin, UNC0642 or MS-275 (Fig. 4*B*).

In addition, we used EPM to test anxiety in $SI^{RS}$ or $GH^{RS}$ mice treated with various drugs. As shown in Fig. 4*C*, romidepsin-treated $SI^{RS}$ mice exhibited a trend of increase in open arm time and distance, but none of the measured parameters were significantly changed. Collectively, these data suggest that HDAC inhibition can ameliorate the

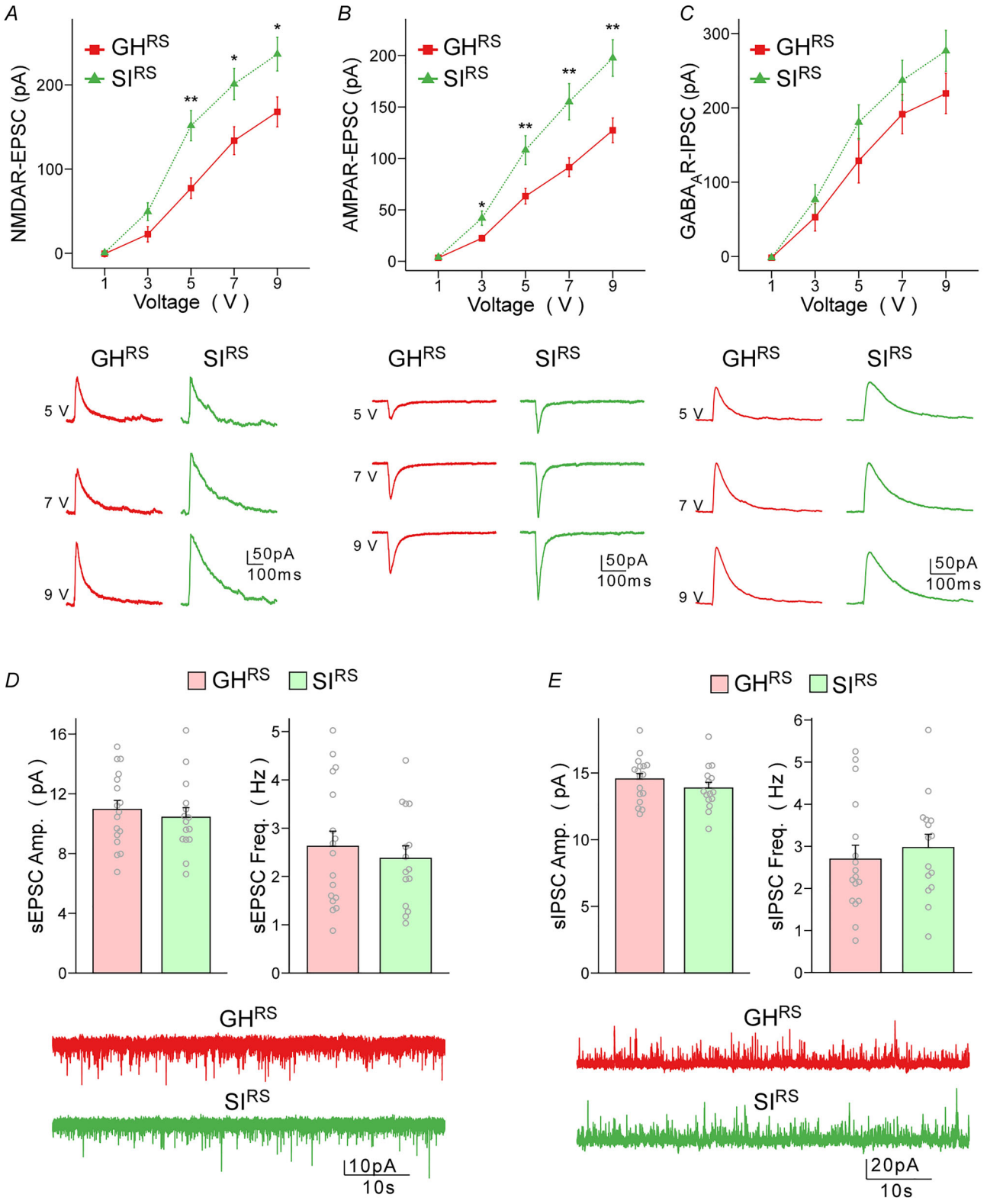


**Figure 2. Socially isolated male mice exposed to acute stress show increased glutamatergic transmission in PFC pyramidal neurons**

*A–C*, input–output curves and representative traces of NMDAR-EPSC (*A*), AMPAR-EPSC (*B*) and $GABA_AR$-IPSC (*C*) in PFC pyramidal neurons from $GH^{RS}$ and $SI^{RS}$ mice ($n$ = 12−19 cells from 12−19 slices in seven mice per group, NMDAR-EPSC: $F_{1,23(group)}$ = 12.9, $P$ = 0.002; AMPAR-EPSC: $F_{1,31(group)}$ = 10.3, $P$ = 0.003; $GABA_AR$-IPSC:

$F_{1,33(group)}$ = 1.8, $P$ = 0.2, two-way repeated-measures ANOVA). *D* and *E*, bar graphs and representative traces of spontaneous EPSC (sEPSC, *D*) and IPSC (sIPSC, *E*) in PFC pyramidal neurons from $GH^{RS}$ and $SI^{RS}$ mice ($n$ = 15−17 cells from 15−17 slices in seven mice per group; sEPSC: Amplitude: $t_{30}$ = 0.6, $P$ = 0.6; Frequency: $t_{30}$ = 0.6, $P$ = 0.6, $t$ test; sIPSC: Amplitude: $t_{30}$ = 1.1, $P$ = 0.3; Frequency: $t_{30}$ = 0.6, $P$ = 0.6, $t$ test). In all figures, $^{*}P < 0.05$, $^{**}P < 0.01$, $^{***}P < 0.001$. All data are expressed as mean ± SEM.

escalated aggressive behaviour, as well as general social interaction deficits, in $SI^{RS}$ mice.

### HDAC inhibition normalizes glutamatergic transmission in socially isolated mice exposed to acute stress

Given the therapeutic effects of HDAC inhibitors on aggressive behaviour of $SI^{RS}$ mice, we next examined whether treatment with romidepsin could reverse synaptic dysfunction in PFC pyramidal neurons. As shown in Fig. 5*A* and *B*, NMDAR-EPSC and AMPAR-EPSC amplitudes in romidepsin-treated $SI^{RS}$ mice ($SI^{RS}$+Rom) were significantly smaller than those in vehicle-treated $SI^{RS}$ mice ($SI^{RS}$+Veh) and were similar to those in vehicle-treated $GH^{RS}$ controls ($GH^{RS}$+Veh).

Romidepsin treatment did not significantly alter $GABA_AR$-IPSC in $SI^{RS}$ mice (Fig. 5*C*). Furthermore, both sEPSC and sIPSC remained largely unchanged after treatment with romidepsin, despite a small but significant increase in the amplitude of sIPSC (Fig. 5*D* and *E*). Together, these results suggest that the abnormally elevated glutamatergic transmission in $SI^{RS}$ mice can be reversed by the inhibition of class I HDAC.

## Discussion

In this study, we have revealed a maladaptive response to acute stress in male mice after chronic post-weaning social isolation – drastically increased aggression. After submitting to a 2 h restraint stress, socially isolated mice were hyper-aroused during aggressive contacts and delivered substantially more attacks in the RI test. Consistently, human and animal data also show that adverse early-life events, such as repeated maternal separation, adolescent social isolation and peripubertal stress, strongly affect emotional responses to conflict and aggressive behaviour in adulthood (Haller et al., 2014). Heightened aggression has been associated with various psychiatric disorders, including post-traumatic stress disorder (Taft et al., 2017) and paranoid schizophrenia (Darrell-Berry et al., 2016). The escalated aggression in socially isolated mice is an indicator of their elevated vulnerability to mental distress and disorders.

Neuroimaging studies suggest that impulsivity and aggression are correlated with frontal and temporal brain abnormalities (Soyka, 2011). Using the activity marker c-Fos, it has been found that post-weaning social isolation in rats submitted to resident–intruder conflicts leads to significantly increased activation of brain areas controlling inter-male aggression, such as the medial and lateral orbitofrontal cortices, anterior cingulate cortex, medial and basolateral amygdala, and hypothalamic paraventricular nucleus (Toth et al., 2012). Our electrophysiological studies have found that SI males after 2 h of restraint stress have significantly larger NMDAR- and AMPAR-mediated synaptic currents in PFC pyramidal neurons, compared to GH counterparts. The hyperactive PFC in response to acute stress could lead to dysregulation of direct and indirect targets of PFC, which contributes to the manifestation of aggressive behaviour (Adams & Rosenkranz, 2016; Tan et al., 2021; Wei et al., 2018).

A potential mechanism for gene–environment interactions in shaping risks for stress-related psychiatric disorders is epigenetic modifications that can lead to prolonged molecular changes (Klengel & Binder, 2015). Mounting evidence has revealed a plethora of epigenetic changes that are induced by various types of stress, which cause aberrant DNA methylation and histone modification at specific genes in target regions including PFC (Sanacora et al., 2022). In blood samples from schizophrenia patients who have encountered early life stress (ELS), the level of HDAC1 is increased (Bahari-Javan et al., 2017). Moreover, *Hdac1* over-expression in mouse PFC neurons mimics schizophrenia-like phenotypes induced by ELS, and systemic administration of an HDAC inhibitor rescues the detrimental effects of ELS (Bahari-Javan et al., 2017). In human subjects with depression and male mice subjected to chronic social defeat stress (CSDS), RAC1, a key regulator of actin cytoskeleton and synaptic structure, shows the reduced transcription, which is associated with a repressive chromatin state surrounding its promoter (Golden et al., 2013). Inhibition of class I HDACs rescues CSDS-induced decrease of RAC1 transcription and depression-related behaviours (Golden et al., 2013). In the current study, we have found the reduced histone acetylation in PFC of SI males exposed to acute restraint stress ($SI^{RS}$), compared to GH counterparts. More importantly, treatment with class I HDAC inhibitors, romidepsin or MS-275, prevented the heightened aggression in $SI^{RS}$ males, while an inhibitor for histone methylation enzymes EHMT1/2 was ineffective. These studies highlight the potential of HDAC inhibition as a therapeutic avenue for stress-associated psychiatric disorders.

To understand the physiological basis of the behavioural impact of HDAC inhibitor in $SI^{RS}$ males,

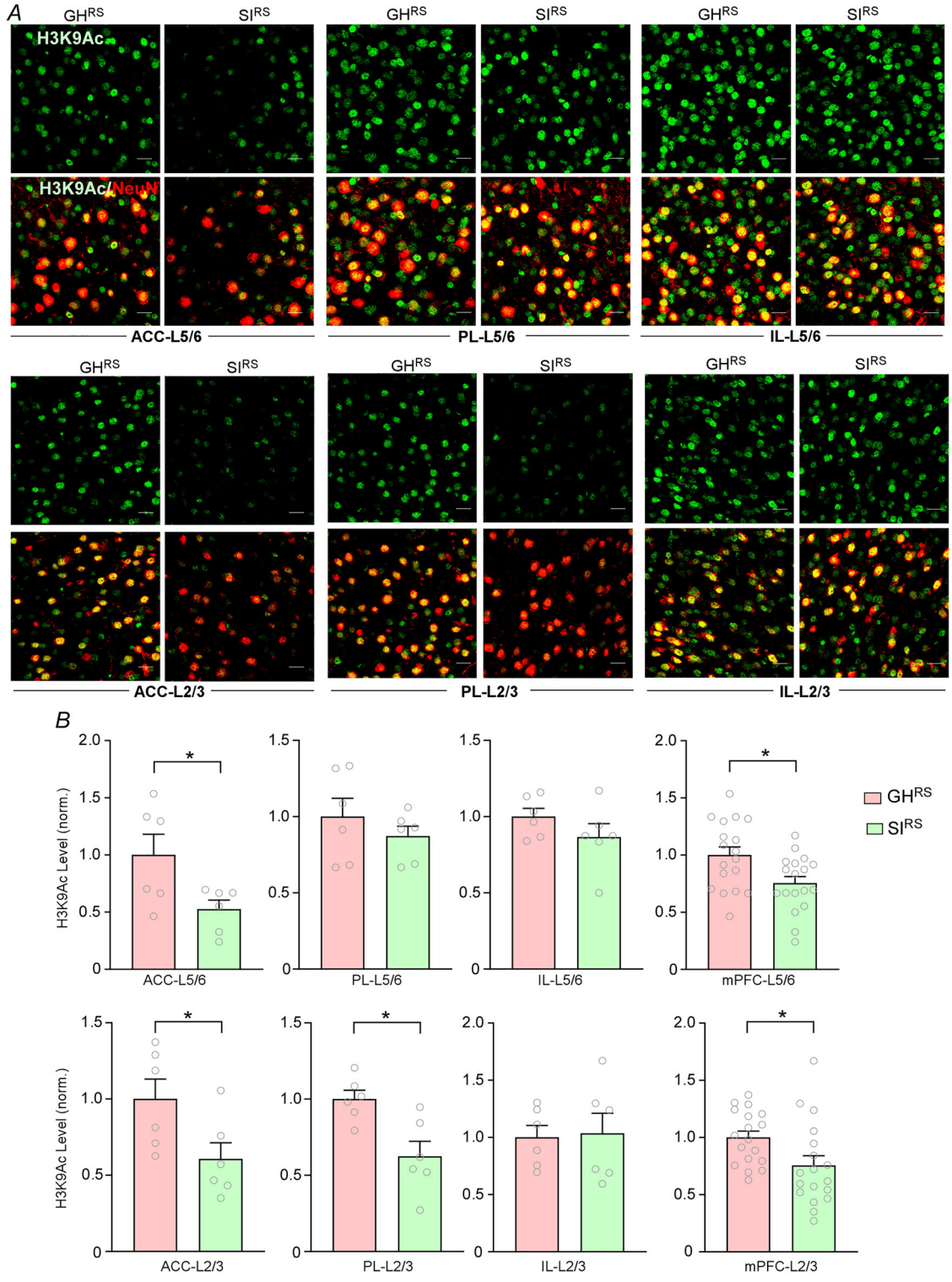


**Figure 3. Histone acetylation is reduced in PFC of socially isolated male mice exposed to acute stress**
*A*, representative confocal images of immunostaining of H3K9Ac (green) and NeuN (red) in different layers of PFC subregions, including ACC-L5/6, ACC-L2/3, PL-L5/6, PL-L2/3, IL-L5/6 and IL-L2/3, of $GH^{RS}$ and $SI^{RS}$ mice. Scale bars: 10 $\mu$m. *B*, quantification of H3K9Ac fluorescence intensity (normalized with NeuN) in different layers of PFC subregions of $GH^{RS}$ and $SI^{RS}$ mice ($n$ = 6 images from six slices in three mice per group). ACC-L5/6, $t_{10}$ = 2.4, $P$ = 0.04; ACC-L2/3, $t_{10}$ = 2.3, $P$ = 0.04; PL-L2/3, $t_{10}$ = 3.3, $P$ = 0.008; mPFC-L5/6, $t_{10}$ = 2.7, $P$ = 0.01; mPFC-L2/3, $t_{10}$ = 2.4, $P$ = 0.02; unpaired $t$ test. In all figures, $^*P < 0.05$. All data are expressed as mean ± SEM.

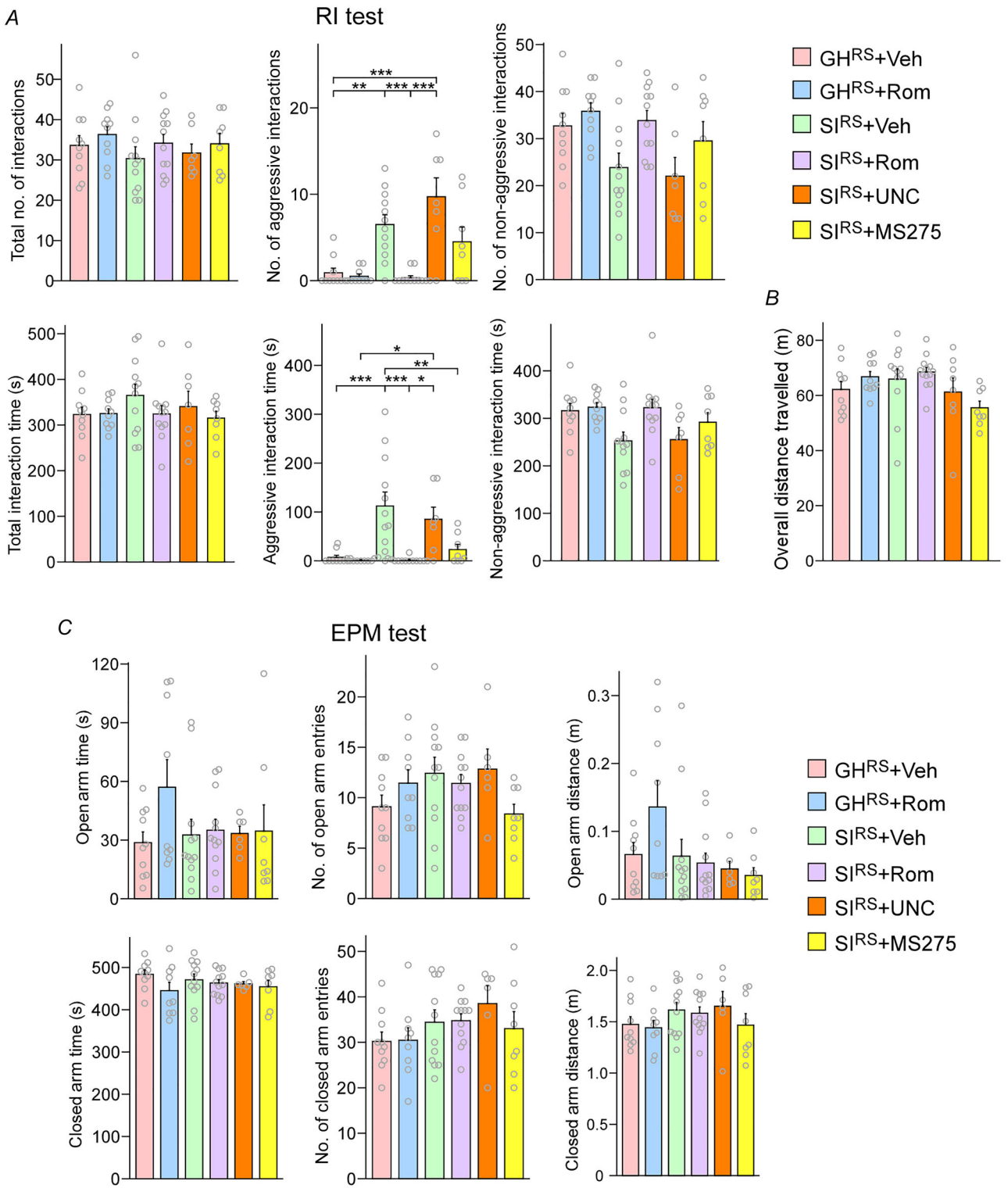


**Figure 4. Treatment with class I HDAC inhibitors ameliorates hyper-aggressive behaviour and general social interaction deficits in socially isolated male mice exposed to acute stress**
*A*, bar graphs showing aggressive behaviour in the resident–intruder (RI) test of $GH^{RS}$ and $SI^{RS}$ mice treated with vehicle, romidepsin, UNC0642 or MS-275 ($n = 7–12$ mice per group; Total no. of interactions: $F_{5,53} = 0.8$, $P = 0.6$; No. of aggressive interactions: $F_{5,53} = 12.3$, $P < 0.0001$; No. of non-aggressive interactions: $F_{5,53} = 3.6$, $P = 0.007$; Total interaction time: $F_{5,53} = 0.9$, $P = 0.5$; Aggressive interaction time: $F_{5,53} = 9.1$, $P < 0.0001$; Non-aggressive interaction time: $F_{5,53} = 3.5$, $P = 0.009$, one-way ANOVA). *B*, bar graph of the overall distance travelled while

performing the RI test ($n$ = 8–13 mice per group, $F_{5,55}$ = 2.27, $P$ = 0.06, one-way ANOVA). *C*, bar graphs of time, distance travelled and number of entries to open arms (OA) and closed arms (CA) for each group in the elevated plus maze (EPM) test ($n$ = 6–12 mice per group, OA time: $F_{5,51}$ = 1.2, $P$ = 0.3; CA time: $F_{5,51}$ = 1.0, $P$ = 0.4; OA distance: $F_{5,51}$ = 2.2, $P$ = 0.07; CA distance: $F_{5,51}$ = 1.0, $P$ = 0.4; OA entries: $F_{5,51}$ = 1.7, $P$ = 0.2; CA entries: $F_{5,51}$ = 1.1, $P$ = 0.4, one-way ANOVA). In all figures, $^{*}P < 0.05$, $^{**}P < 0.01$, $^{***}P < 0.001$. All data are expressed as mean ± SEM.

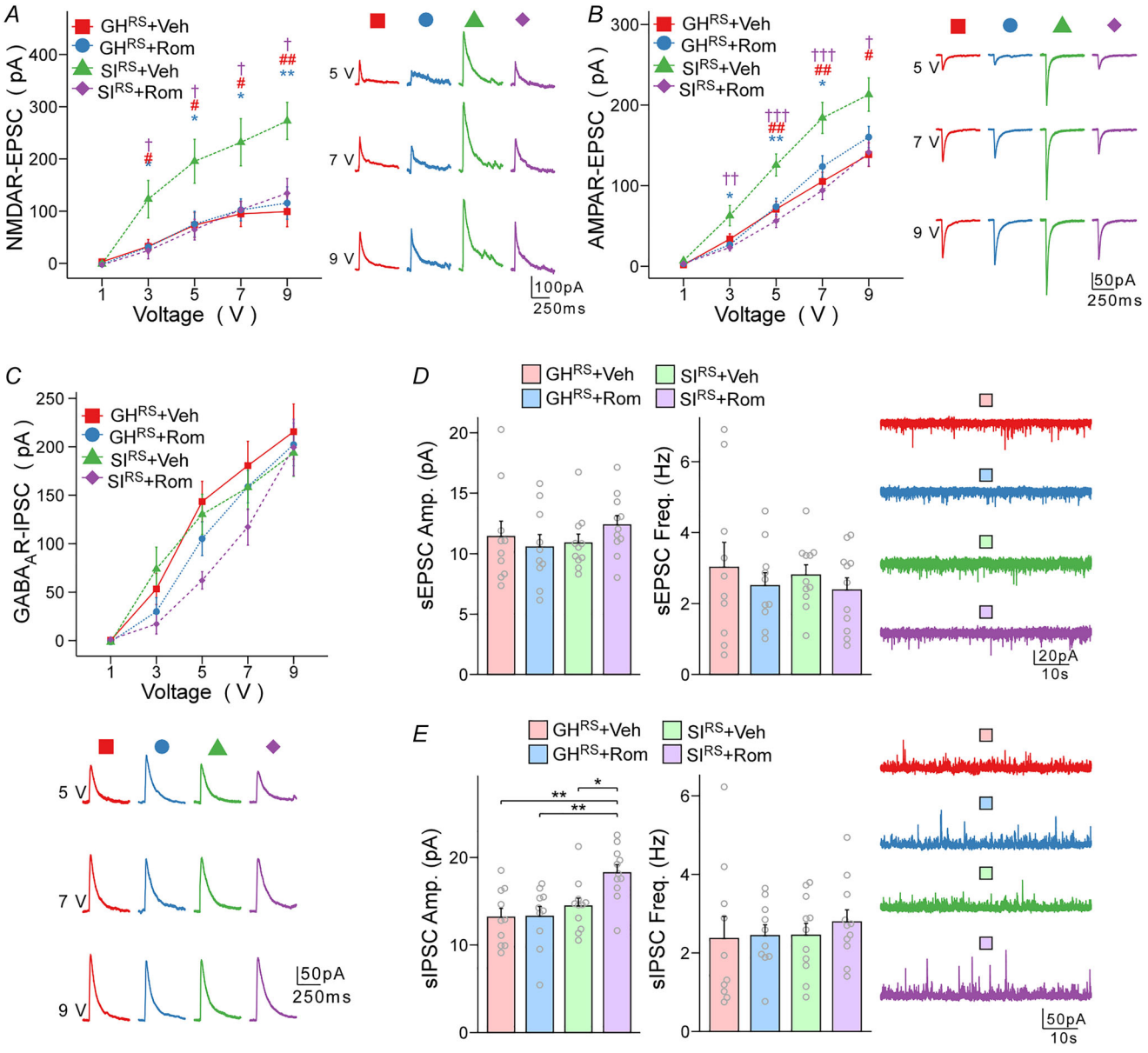


**Figure 5. HDAC inhibition normalizes glutamatergic transmission in PFC pyramidal neurons from socially isolated male mice exposed to acute stress**
*A–C*, input–output curves and representative traces of NMDAR-EPSC (*A*), AMPAR-EPSC (*B*) and $GABA_AR$-IPSC (*C*) in PFC pyramidal neurons from $GH^{RS}$ and $SI^{RS}$ mice treated with vehicle or romidepsin ($n$ = 7–11 cells from

we examined its effect on PFC glutamatergic transmission, which mediates emotional and cognitive processes subserved by PFC (Yan & Rein, 2022). We have revealed that the abnormally elevated NMDAR-EPSC and AMPAR-EPSC in PFC pyramidal neurons of $SI^{RS}$ males are reversed by romidepsin treatment, suggesting the normalization of neuronal activity in PFC and its target regions by HDAC inhibition. Taken together, this study has revealed an epigenetic mechanism that may be causally linked to aberrant responses to acute

7–11 slices in 6–7 mice per group, NMDAR-EPSC: $F_{3,24(group)} = 8.0$, $P = 0.0007$; AMPAR-EPSC: $F_{3,36(group)} = 7.6$, $P = 0.0004$; $GABA_AR$-IPSC: $F_{1,35(group)} = 1.6$, $P = 0.2$, two-way repeated-measures ANOVA). $^{\#}P < 0.05$, $^{\#\#}P < 0.01$, $^{\#\#\#}P < 0.001$, SI+Veh *versus* GH+Veh; $^{*}P < 0.05$, $^{**}P < 0.01$, $^{***}P < 0.001$, SI+Veh *versus* GH+Rom; $^{\dagger}P < 0.05$, $^{\dagger\dagger}P < 0.01$, $^{\dagger\dagger\dagger}P < 0.001$, SI+Veh *versus* SI+Rom. *D* and *E*, bar graphs of amplitude and frequency of sEPSC (*D*) and sIPSC (*E*) in PFC pyramidal neurons from vehicle- or romidepsin-treated $GH^{RS}$ or $SI^{RS}$ mice ($n$ = 10–11 cells from 10–11 slices in 6–7 mice per group, sEPSC: Amplitude: $F_{3,38} = 0.7$, $P = 0.6$, Frequency: $F_{3,38} = 0.4$, $P = 0.7$; sIPSC: Amplitude: $F_{3,38} = 6.0$, $P = 0.002$, Frequency: $F_{3,38} = 0.3$, $P = 0.9$, one-way ANOVA). Inset: representative traces. All data are expressed as mean ± SEM.

stress in male mice exposed to adolescent isolation stress.

## References


Adams, T., & Rosenkranz, J. A. (2016). Social isolation during postweaning development causes hypoactivity of neurons in the medial nucleus of the male rat amygdala. *Neuropsychopharmacology*, **41**(7), 1929–1940.

Almeida, I. L. L., Rego, J. F., Teixeira, A. C. G., & Moreira, M. R. (2021). Social isolation and its impact on child and adolescent development: A systematic review. *Revista Paulista de Pediatria: Orgao Oficial da Sociedade de Pediatria de Sao Paulo*, **40**, e2020385.

Bahari-Javan, S., Varbanov, H., Halder, R., Benito, E., Kaurani, L., Burkhardt, S., Anderson-Schmidt, H., Anghelescu, I., Budde, M., Stilling, R. M., Costa, J., Medina, J., Dietrich, D. E., Figge, C., Folkerts, H., Gade, K., Heilbronner, U., Koller, M., Konrad, C., … Fischer, A. (2017). HDAC1 links early life stress to schizophrenia-like phenotypes. *PNAS*, **114**(23), E4686–E4694.

Barnett Burns, S., Almeida, D., & Turecki, G. (2018). The epigenetics of early life adversity: Current limitations and possible solutions. *Progress in Molecular Biology and Translational Science*, **157**, 343–425.

Bradski, G. (2000). The OpenCV Library. Dr Dobb's Journal of Software Tools.

Chang, C.-H., Hsiao, Y.-H., Chen, Y.-W., Yu, Y.-J., & Gean, P.-W. (2015). Social isolation-induced increase in NMDA receptors in the hippocampus exacerbates emotional dysregulation in mice. *Hippocampus*, **25**(4), 474–485.

Chang, C.-H., Su, C.-L., & Gean, P.-W. (2018). Mechanism underlying NMDA blockade-induced inhibition of aggression in post-weaning socially isolated mice. *Neuropharmacology*, **143**, 95–105.

Covington, H. E., 3rd, Maze, I., LaPlant, Q. C., Vialou, V. F., Ohnishi, Y. N., Berton, O., Fass, D. M., Renthal, W., Rush, A. J., 3rd, Wu, E. Y., Ghose, S., Krishnan, V., Russo, S. J., Tamminga, C., Haggarty, S. J., & Nestler, E. J. (2009). Antidepressant actions of histone deacetylase inhibitors. *Journal of Neuroscience*, **29**(37), 11451–11460.

Darrell-Berry, H., Berry, K., & Bucci, S. (2016). The relationship between paranoia and aggression in psychosis: A systematic review. *Schizophrenia Research*, **172**(1–3), 169–176.

Garcia, S., Guarino, D., Jaillet, F., Jennings, T., Pröpper, R., Rautenberg, P., Rodgers, C., Sobolev, A., Wachtler, T., Yger, P., & Davison, A. P. (2014). Neo: An object model for handling electrophysiology data in multiple formats. *Frontiers in Neuroinformatics*, **8**, 10.

Golden, S. A., Christoffel, D. J., Heshmati, M., Hodes, G. E., Magida, J., Davis, K., Cahill, M. E., Dias, C., Ribeiro, E., Ables, J. L., Kennedy, P. J., Robison, A. J., Gonzalez-Maeso, J., Neve, R. L., Turecki, G., Ghose, S., Tamminga, C. A., & Russo, S. J. (2013). Epigenetic regulation of RAC1 induces synaptic remodeling in stress disorders and depression. *Nature Medicine*, **19**(3), 337–344.

Haller, J., Harold, G., Sandi, C., & Neumann, I. D. (2014). Effects of adverse early-life events on aggression and anti-social behaviours in animals and humans. *Journal of Neuroendocrinology*, **26**(10), 724–738.

Hawkley, L. C., & Cacioppo, J. T. (2010). Loneliness matters: A theoretical and empirical review of consequences and mechanisms. *Annals of Behavioral Medicine*, **40**(2), 218–227.

Holz, N. E., Berhe, O., Sacu, S., Schwarz, E., Tesarz, J., Heim, C. M., & Tost, H. (2023). Early social adversity, altered brain functional connectivity, and mental health. *Biological Psychiatry*, **93**(5), 430–441.

Kassambara, A. (2022). rstatix: Pipe-Friendly Framework for Basic Statistical Tests.

Kendler, K. S., Karkowski, L. M., & Prescott, C. A. (1999). Causal relationship between stressful life events and the onset of major depression. *American Journal of Psychiatry*, **156**(6), 837–841.

Klengel, T., & Binder, E. B. (2015). Epigenetics of stress-related psychiatric disorders and gene × environment interactions. *Neuron*, **86**(6), 1343–1357.

Koolhaas, J. M., Coppens, C. M., Boer, S. F. D., Buwalda, B., Meerlo, P., & Timmermans, P. J. A. (2013). The resident-intruder paradigm: A standardized test for aggression, violence and social stress. *JoVE (Journal of Visualized Experiments)*, (77), e4367.

Lukkes, J., Watt, M., Lowry, C., & Forster, G. (2009). Consequences of post-weaning social isolation on anxiety behavior and related neural circuits in rodents. *Frontiers in Behavioral Neuroscience*, **3**, 18.

Ma, K., Qin, L., Matas, E., Duffney, L. J., Liu, A., & Yan, Z. (2018). Histone deacetylase inhibitor MS-275 restores social and synaptic function in a Shank3-deficient mouse model of autism. *Neuropsychopharmacology*, **43**(8), 1779–1788.

Miczek, K. A., Maxson, S. C., Fish, E. W., & Faccidomo, S. (2001). Aggressive behavioral phenotypes in mice. *Behavioural Brain Research*, **125**(1–2), 167–181.

Nelson, R. J., & Trainor, B. C. (2007). Neural mechanisms of aggression. *Nature Reviews Neuroscience*, **8**(7), 536–546.

Nemeroff, C. B. (2016). Paradise lost: The neurobiological and clinical consequences of child abuse and neglect. *Neuron*, **89**(5), 892–909.

Nordman, J., Ma, X., & Li, Z. (2020). Traumatic stress induces prolonged aggression increase through synaptic potentiation in the medial amygdala circuits. *eNeuro*, **7**(4), ENEURO.0147-20.2020.

Qin, L., Ma, K., Wang, Z.-J., Hu, Z., Matas, E., Wei, J., & Yan, Z. (2018). Social deficits in Shank3-deficient mouse models of autism are rescued by histone deacetylase (HDAC) inhibition. *Nature Neuroscience*, **21**(4), 564–575.

Rahman, M. F., & McGowan, P. O. (2022). Cell-type-specific epigenetic effects of early life stress on the brain. *Translational Psychiatry*, **12**(1), 326.

Sanacora, G., Yan, Z., & Popoli, M. (2022). The stressed synapse 2.0: Pathophysiological mechanisms in stress-related neuropsychiatric disorders. *Nature Reviews Neuroscience*, **23**(2), 86–103.

Siuda, D., Wu, Z., Chen, Y., Guo, L., Linke, M., Zechner, U., Xia, N., Reifenberg, G., Kleinert, H., Forstermann, U., & Li, H. (2014). Social isolation-induced epigenetic changes in midbrain of adult mice. *Journal of Physiology and Pharmacology*, **65**(2), 247–255.

Snyder-Mackler, N., Burger, J. R., Gaydosh, L., Belsky, D. W., Noppert, G. A., Campos, F. A., Bartolomucci, A., Yang, Y. C., Aiello, A. E., O'Rand, A., Harris, K. M., Shively, C. A., Alberts, S. C., & Tung, J. (2020). Social determinants of health and survival in humans and other animals. *Science*, **368**(6493), eaax9553.

Soyka, M. (2011). Neurobiology of aggression and violence in schizophrenia. *Schizophrenia Bulletin*, **37**(5), 913–920.

Strahl, B. D., & Allis, C. D. (2000). The language of covalent histone modifications. *Nature*, **403**(6765), 41–45.

Taft, C. T., Creech, S. K., & Murphy, C. M. (2017). Anger and aggression in PTSD. *Current Opinion in Psychology*, **14**, 67–71.

Tan, T., Wang, W., Liu, T., Zhong, P., Conrow-Graham, M., Tian, X., & Yan, Z. (2021). Neural circuits and activity dynamics underlying sex-specific effects of chronic social isolation stress. *Cell Reports*, **34**(12), 108874.

Tan, T., Wang, W., Williams, J., Ma, K., Cao, Q., & Yan, Z. (2019). Stress exposure in dopamine D4 receptor knockout mice induces schizophrenia-like behaviors via disruption of GABAergic transmission. *Schizophrenia Bulletin*, **45**(5), 1012–1023.

Toth, M., Tulogdi, A., Biro, L., Soros, P., Mikics, E., & Haller, J. (2012). The neural background of hyper-emotional aggression induced by post-weaning social isolation. *Behavioural Brain Research*, **233**(1), 120–129.

Uchida, S., Hara, K., Kobayashi, A., Otsuki, K., Yamagata, H., Hobara, T., Suzuki, T., Miyata, N., & Watanabe, Y. (2011). Epigenetic status of Gdnf in the ventral striatum determines susceptibility and adaptation to daily stressful events. *Neuron*, **69**(2), 359–372.

Walf, A. A., & Frye, C. A. (2007). The use of the elevated plus maze as an assay of anxiety-related behavior in rodents. *Nature Protocols*, **2**(2), 322–328.

Waltes, R., Chiocchetti, A. G., & Freitag, C. M. (2016). The neurobiological basis of human aggression: A review on genetic and epigenetic mechanisms. *American Journal of Medical Genetics Part B: Neuropsychiatric Genetics*, **171**(5), 650–675.

Wang, W., Cao, Q., Tan, T., Yang, F., Williams, J. B., & Yan, Z. (2021). Epigenetic treatment of behavioral and physiological deficits in a tauopathy mouse model. *Aging Cell*, **20**(10), e13456.

Wang, W., Rein, B., Zhang, F., Tan, T., Zhong, P., Qin, L., & Yan, Z. (2018). Chemogenetic activation of prefrontal cortex rescues synaptic and behavioral deficits in a mouse model of 16p11.2 deletion syndrome. *Journal of Neuroscience*, **38**(26), 5939–5948.

Wang, Z. J., Shwani, T., Liu, J., Zhong, P., Yang, F., Schatz, K., Zhang, F., Pralle, A., & Yan, Z. (2022). Molecular and cellular mechanisms for differential effects of chronic social isolation stress in males and females. *Molecular Psychiatry*, **27**(7), 3056–3068.

Wei, J., Zhong, P., Qin, L., Tan, T., & Yan, Z. (2018). Chemicogenetic restoration of the prefrontal cortex to amygdala pathway ameliorates stress-induced deficits. *Cerebral Cortex*, **28**(6), 1980–1990.

Wu, H., & Zhang, Y. (2014). Reversing DNA methylation: Mechanisms, genomics, and biological functions. *Cell*, **156**(1–2), 45–68.

Yan, Z., & Rein, B. (2022). Mechanisms of synaptic transmission dysregulation in the prefrontal cortex: Pathophysiological implications. *Molecular Psychiatry*, **27**(1), 445–465.

Zelikowsky, M., Hui, M., Karigo, T., Choe, A., Yang, B., Blanco, M. R., Beadle, K., Gradinaru, V., Deverman, B. E., & Anderson, D. J. (2018). The neuropeptide Tac2 controls a distributed brain state induced by chronic social isolation stress. *Cell*, **173**(5), 1265–1279. e19.

Zhang, F., Rein, B., Zhong, P., Shwani, T., Conrow-Graham, M., Wang, Z.-J., & Yan, Z. (2021). Synergistic inhibition of histone modifiers produces therapeutic effects in adult Shank3-deficient mice. *Translational Psychiatry*, **11**(1), 99.

Zhang, Z., Zhang, Y., Yuwen, T., Huo, J., Zheng, E., Zhang, W., & Li, J. (2022). Hyper-excitability of corticothalamic PT neurons in mPFC promotes irritability in the mouse model of Alzheimer's disease. *Cell Reports*, **41**(5), 111577.

Zheng, Y., Liu, A., Wang, Z.-J., Cao, Q., Wang, W., Lin, L., Ma, K., Zhang, F., Wei, J., Matas, E., Cheng, J., Chen, G. J., Wang, X., & Yan, Z. (2019). Inhibition of EHMT1/2 rescues synaptic and cognitive functions for Alzheimer's disease. *Brain*, **142**(3), 787–807.

Zhong, P., Cao, Q., & Yan, Z. (2022). Selective impairment of circuits between prefrontal cortex glutamatergic neurons and basal forebrain cholinergic neurons in a tauopathy mouse model. *Cerebral Cortex*, **32**(24), 5569–5579.

## Additional information

### Data availability statement

Data will be made available on request.

### Competing interests

The authors declare no competing interests.

## Author contributions

L.H.C. performed behavioural assays and electrophysiological experiments, and wrote a draft. P.L. and R.S. performed immunostaining experiments. Z.Y. designed experiments, supervised the project and wrote the paper.


## Funding

HHS | NIH | Office of Extramural Research (OER): MH126443.

## Acknowledgements

We thank Xiaoqing Chen for her excellent technical support. This work was supported by a grant from the National Institutes of Health (R01-MH126443) to Z.Y.

## Keywords

aggression, epigenetics, excitatory synaptic transmission, histone deacetylase, patch clamp, prefrontal cortex, social isolation, stress


## Supporting information

Additional supporting information can be found online in the Supporting Information section at the end of the HTML view of the article. Supporting information files available:

**Peer Review History**